Supporting Information for

Pontederia crassipes inspired bottom overflow for fast and stable drainage

Can Gao,[ab] Chengqi Zhang,[a] Shijie Liu,[ab] Cunlong Yu,[a] Lei Jiang,[*ab] and Zhichao Dong[*ab]

[a]CAS Key Laboratory of Bio-inspired Materials and Interfacial Science, Technical Institute of Physics and Chemistry, Chinese Academy of Sciences, Beijing 100190, P. R. China.

[b]School of Future Technology, University of Chinese Academy of Sciences, Beijing 100049, P. R. China.

*Corresponding author

E-mail: dongzhichao@mail.ipc.ac.cn; jianglei@iccas.ac.cn

This PDF file includes:

Scheme S1

Figs. S1-S15

Captions for Movies S1 to S4

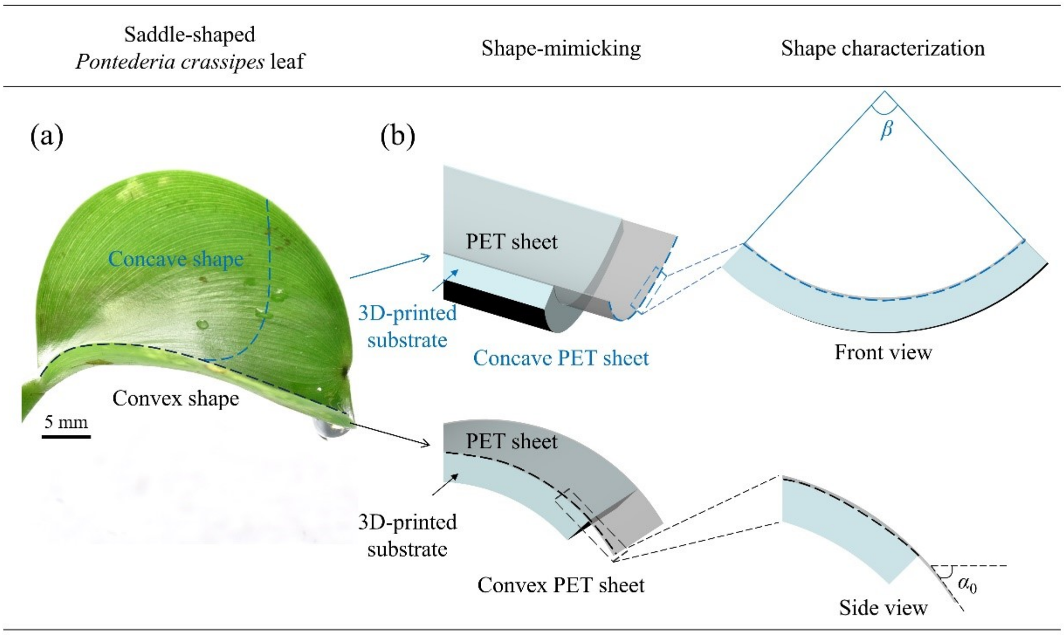

Scheme S1. Biomimetic design inspired by the saddle shape of the *Pontederia crassipes* leaf. (a) *Pontederia crassipes* leaf shows a saddle shape. (b) Schematic diagrams of the shape-mimicking.

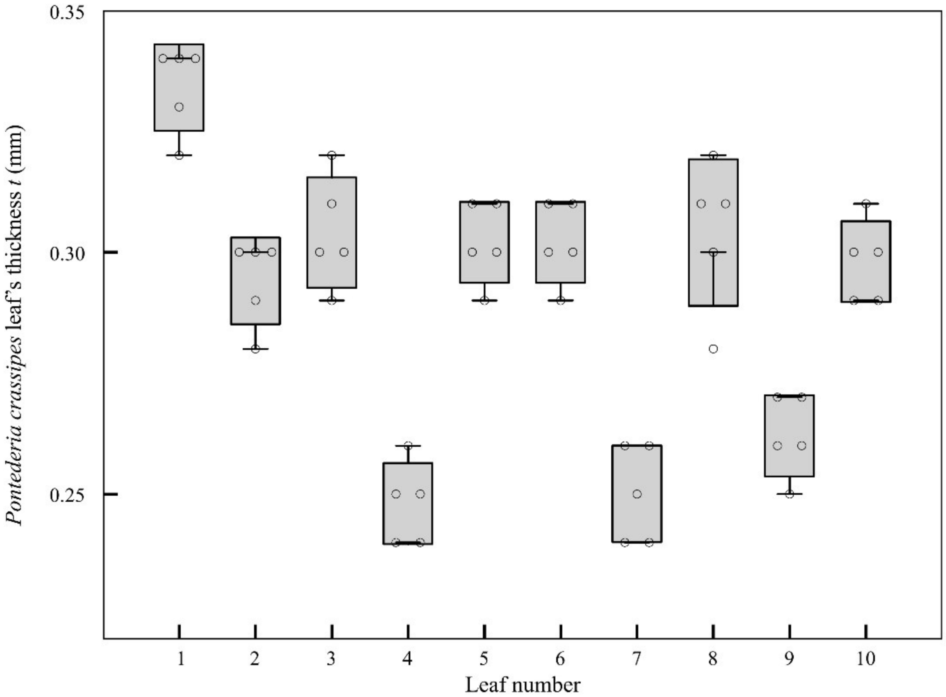

Fig. S1. Thickness distribution of *Pontederia crassipes* leaf. Ten leaves with five positions in every leaf are chosen to count the thickness. The error bars are the ± SD (n = 5).

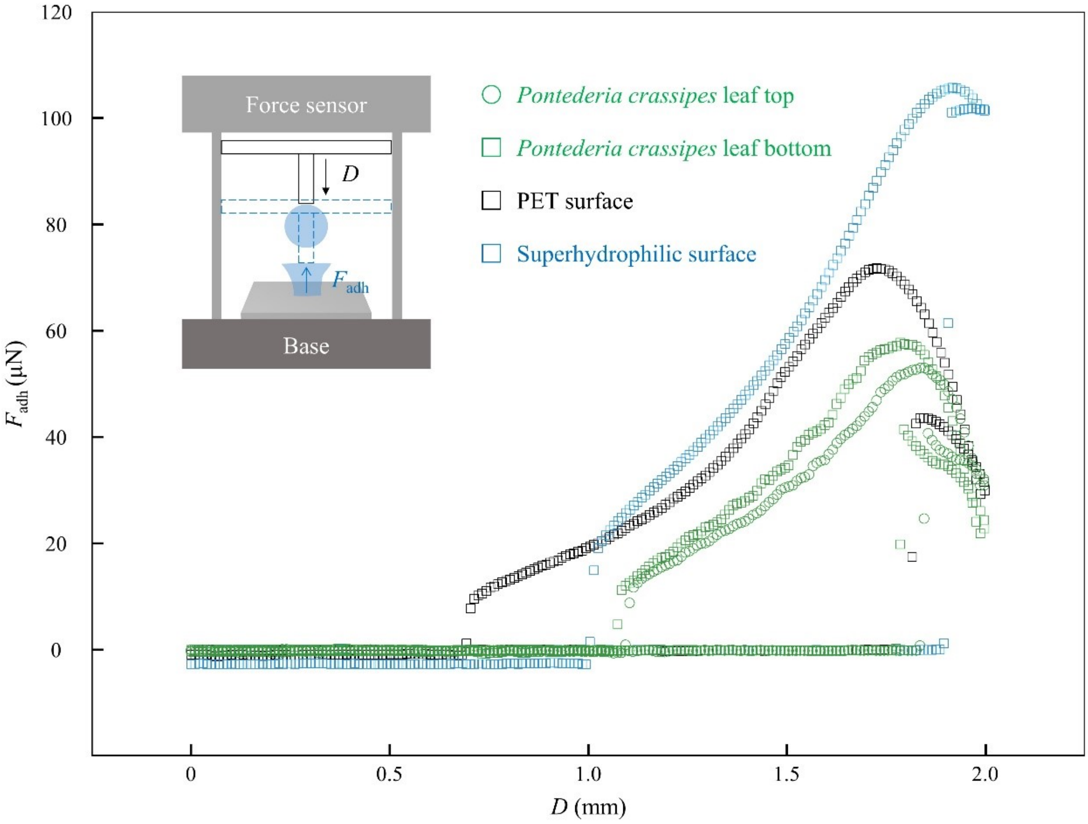

Fig. S2. Adhesion forces of different surfaces with water. Adhesion forces F_{adh} of top and bottom surfaces of *Pontederia crassipes* leaf, PET surface, and superhydrophilic surface with water, respectively.

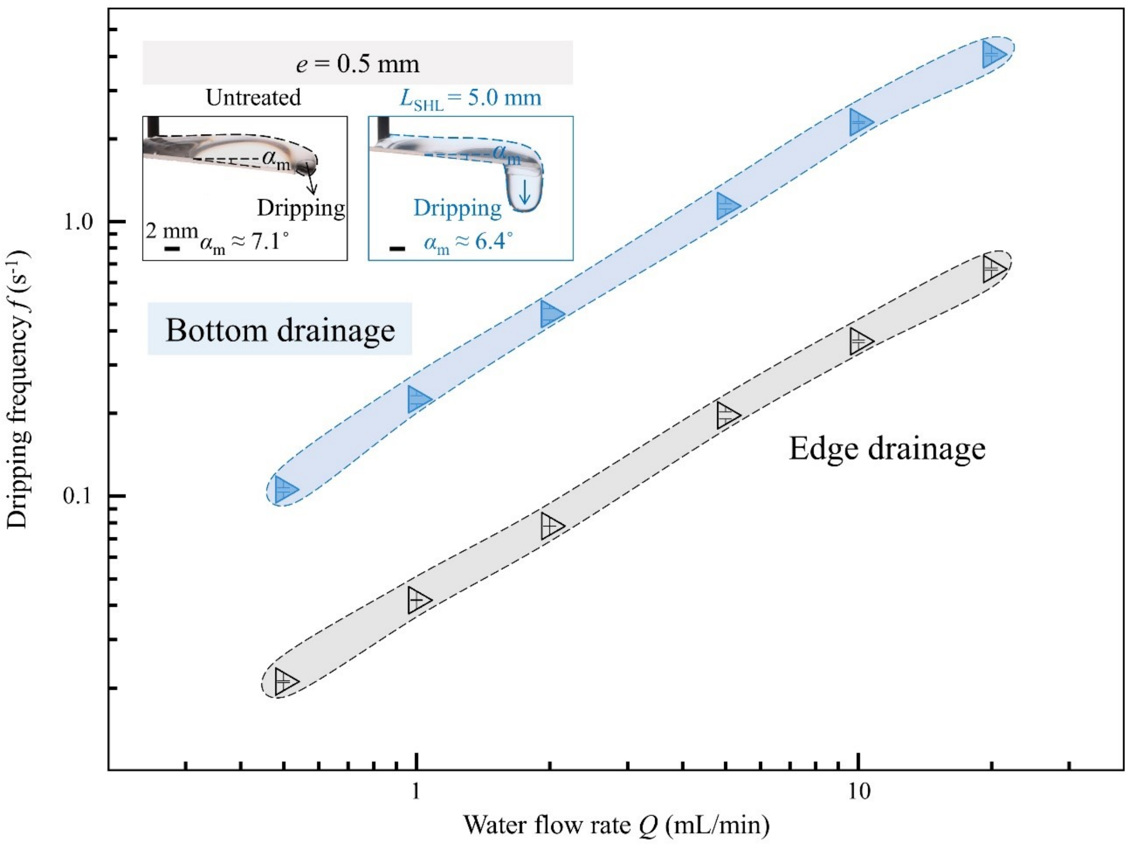

Fig. S3. Dripping frequency versus water flow rate for PET sheets with thickness *e* = 0.5 mm of untreated one and treated one with L_{SHL} = 5.0 mm.

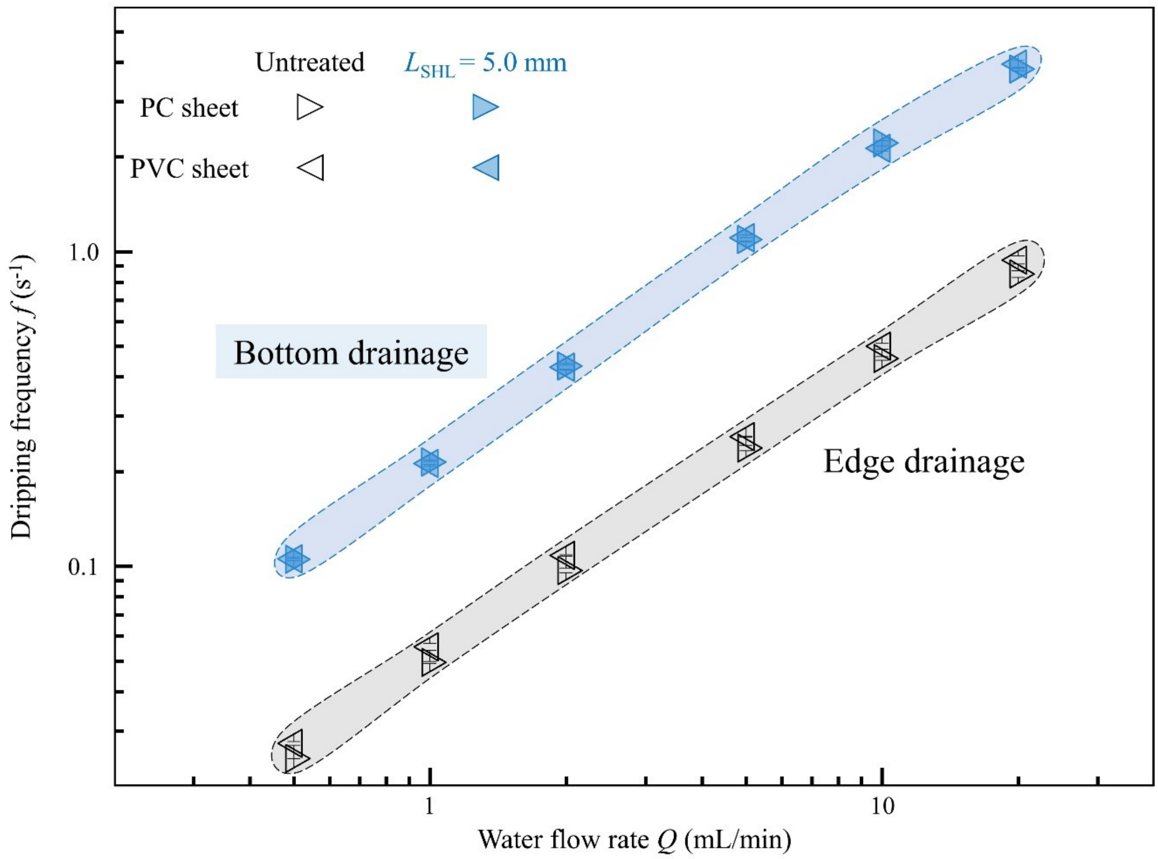

Fig. S4. Dripping frequency versus water flow rate for PVC and PC sheets of untreated ones and treated ones with L_{SHL} = 5.0 mm.

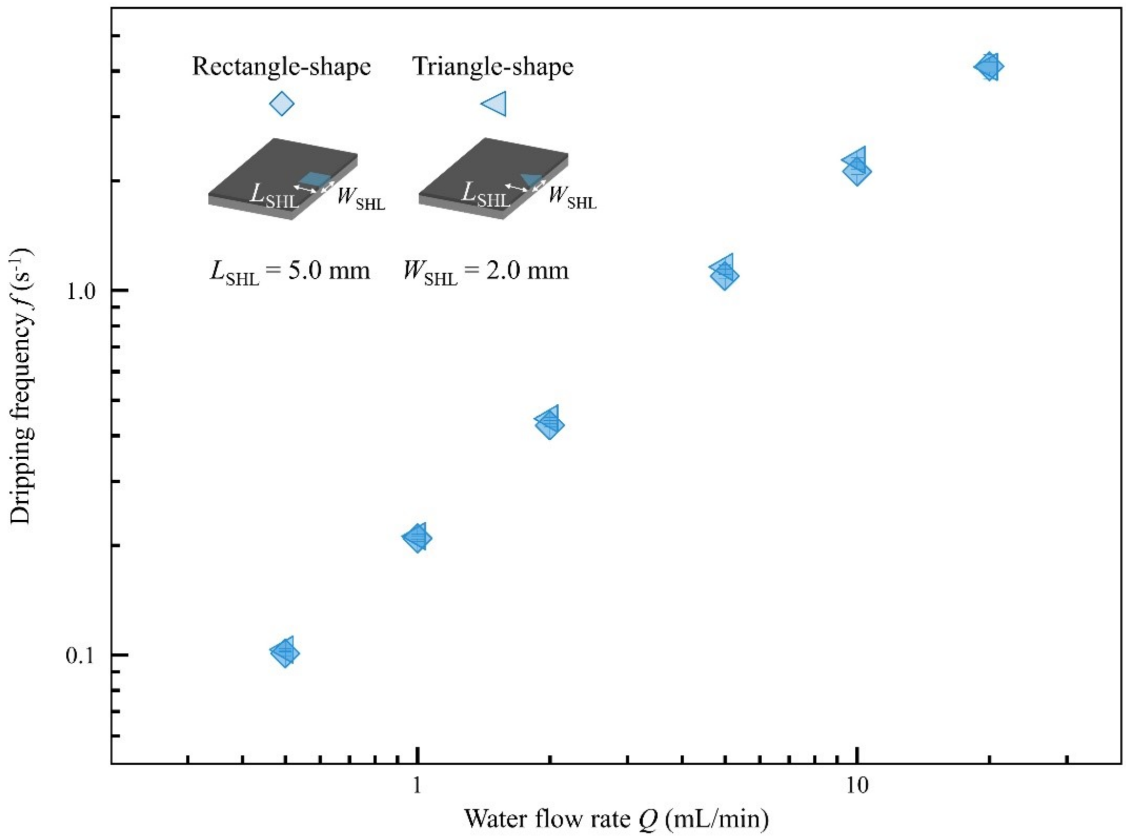

Fig. S5. Comparison of dripping frequency versus water flow rate of PET sheets with treated rectangle- and triangle-shape superhydrophilic zone. The two zones possess the same superhydrophilic length L_{SHL} of 5.0 mm and W_{SHL} of 2.0 mm.

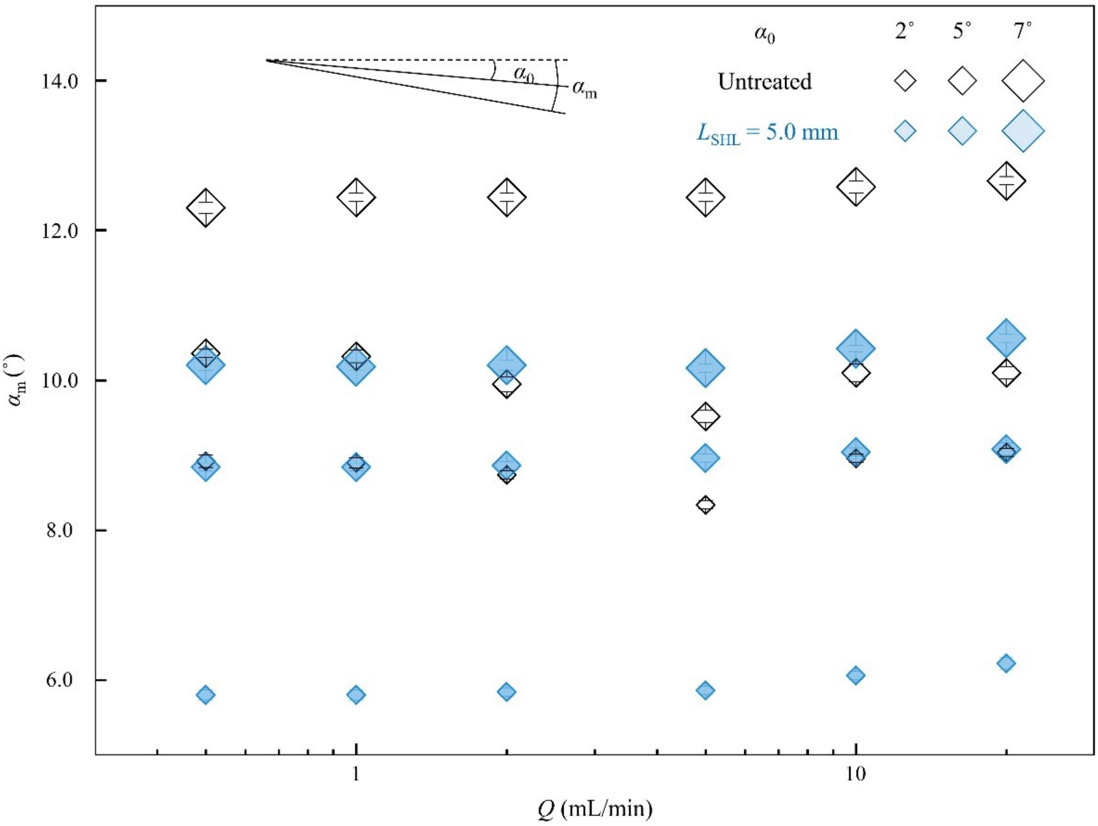

Fig. S6. The maximum dripping angles α_m versus water flow rates Q for the untreated PET and PET with bottom L_{SHL} = 5.0 mm treatment at different α_0. All error bars are the ± SD (n = 5) and they are smaller than the symbols.

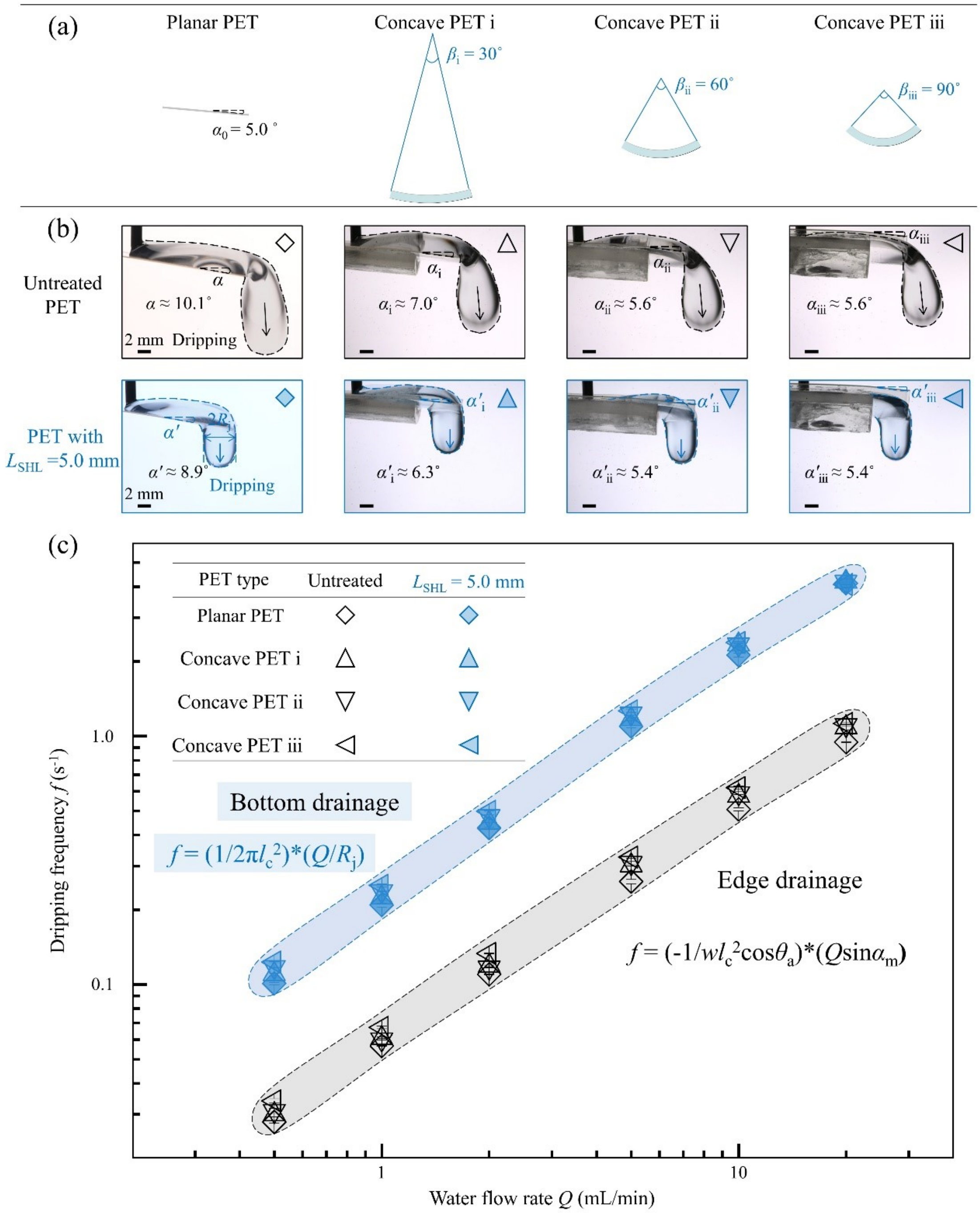

Fig. S7. Drainage frequency comparisons of the planar and concave PET sheets. (a) Schematic diagrams of planar and concave PET sheets. (b-c) Selected critical dripping snapshots (b) and drainage frequency versus water flow rates (c) for PET sheets with different shapes of untreated ones and treated ones with L_{SHL} =5.0 mm.

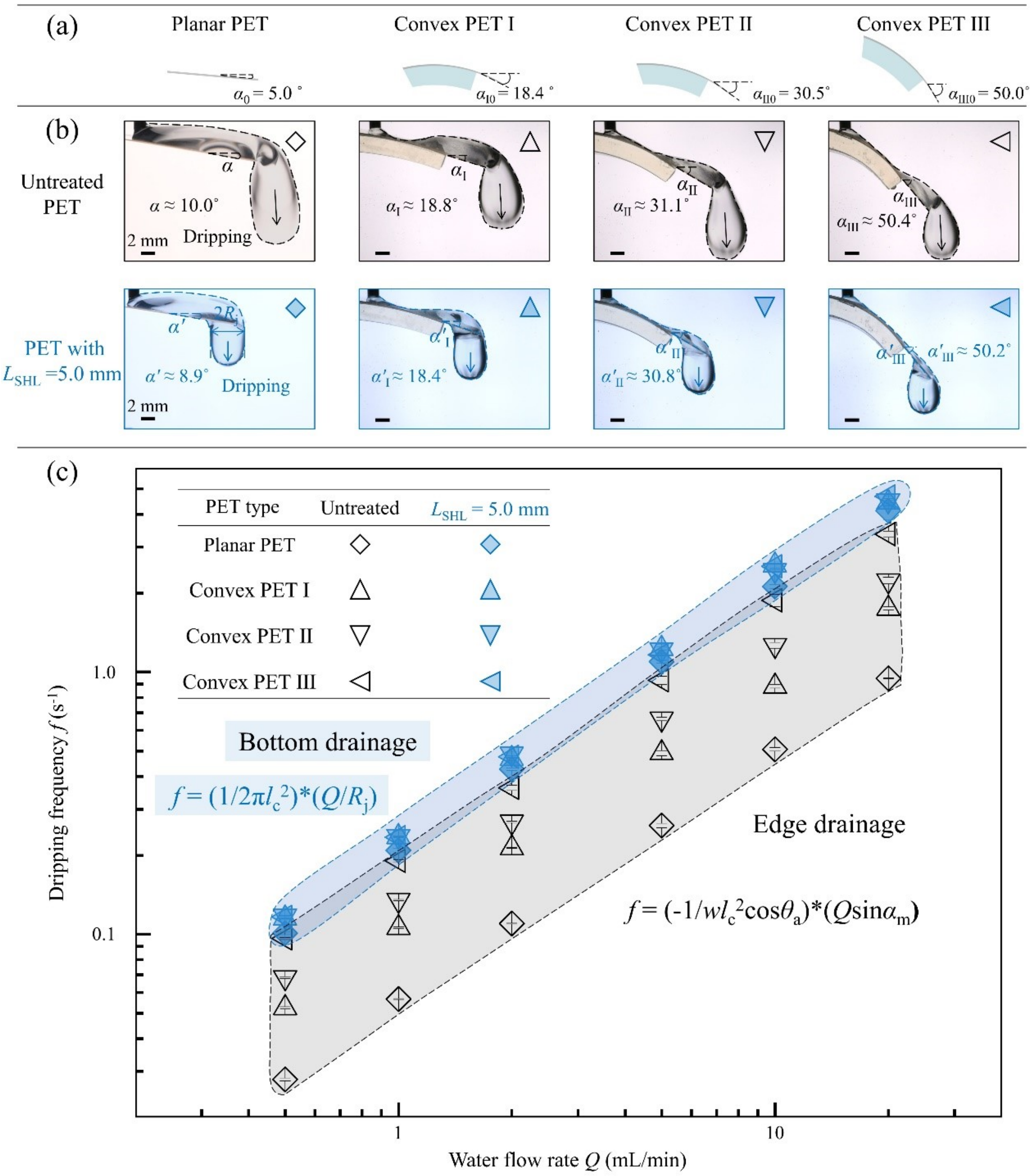

Fig. S8. Drainage result comparisons of planar and convex PET sheets. (a) Schematic diagrams of planar and convex PET sheets. (b-c) Selected critical dripping snapshots (b) and drainage frequency versus water flow rates (c) for PET sheets with different shapes of untreated ones and treated ones with L_{SHL} =5.0 mm.

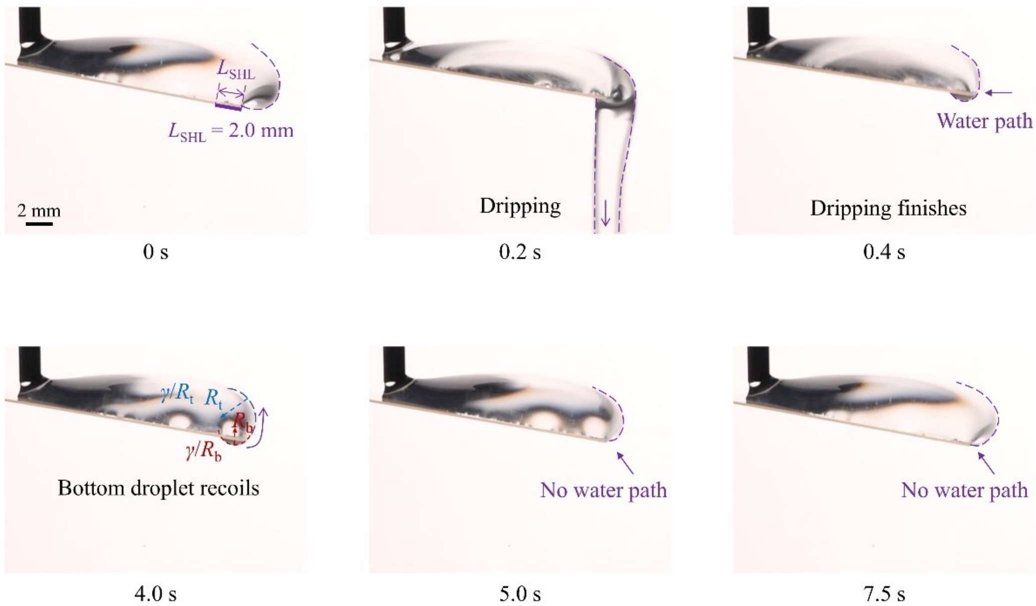

Fig. S9. One drainage process for PET sheet with bottom L_{SHL} = 2.0 mm. The smaller bottom droplet recoils back to the top due to the local pressure gradient ($\gamma/R_b - \gamma/R_t$) and no water path exists after the dripping.

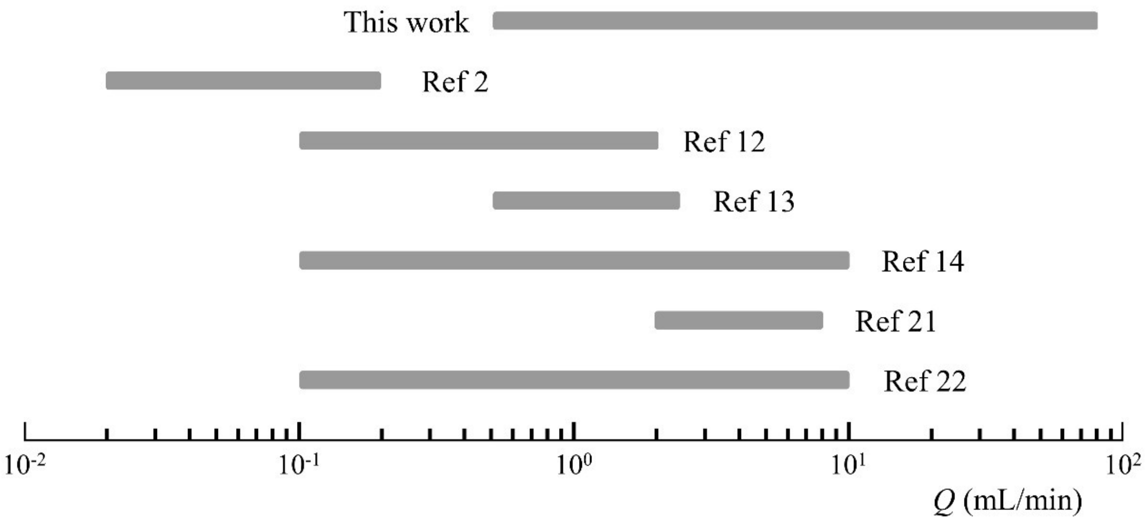

Fig. S10. Comparison of drainage efficiency in this work with other drainage strategies.

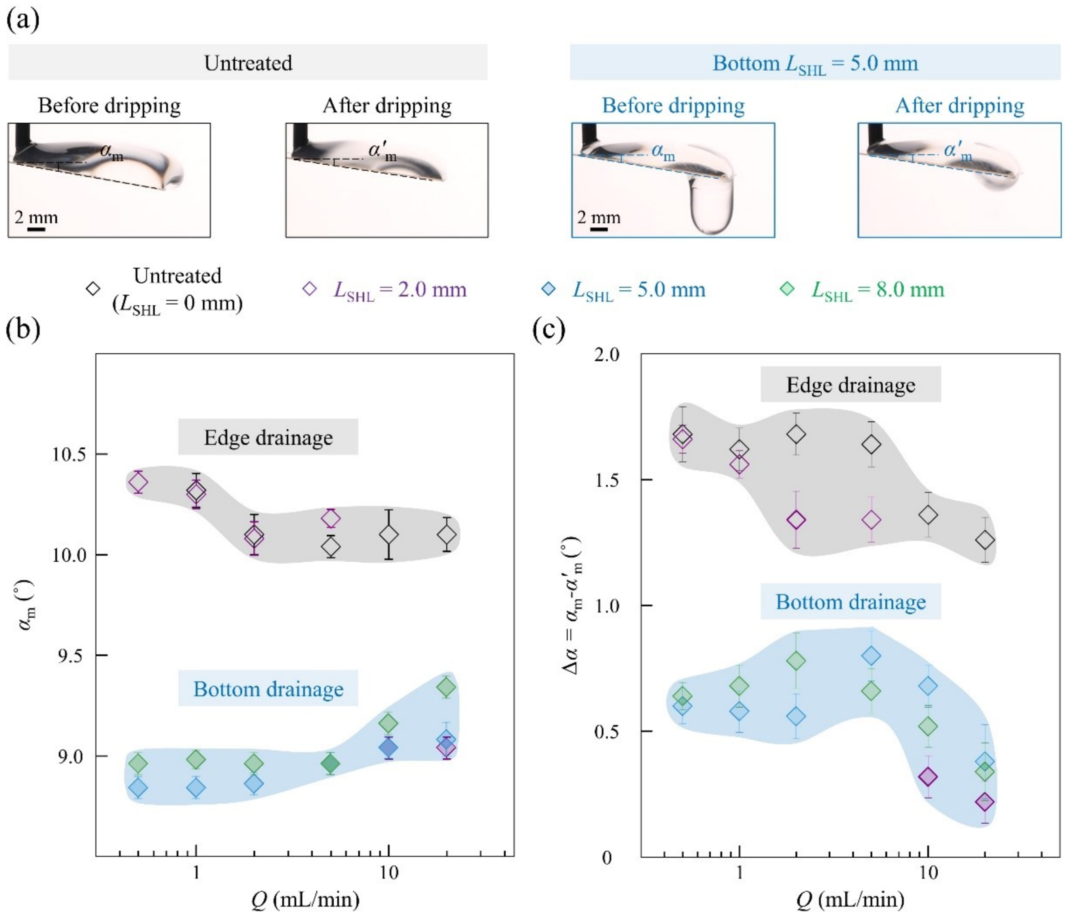

Fig. S11. Dripping angle comparisons of PET sheets. (a) Selected snapshots before and after dripping for the untreated PET and PET with bottom L_{SHL} = 5.0 mm treatment. We define the dripping angle deviation $\Delta\alpha = \alpha_m - \alpha'_m$. Here, α_m represents the maximum dripping angle before dripping and α'_m represents the dripping angle after dripping. (b and c) The maximum dripping angle α_m (b) and dripping angle deviation $\Delta\alpha$ (c) versus water flow rates Q for PET sheets with different bottom L_{SHL} treatments. All error bars are the ± SD (n = 5).

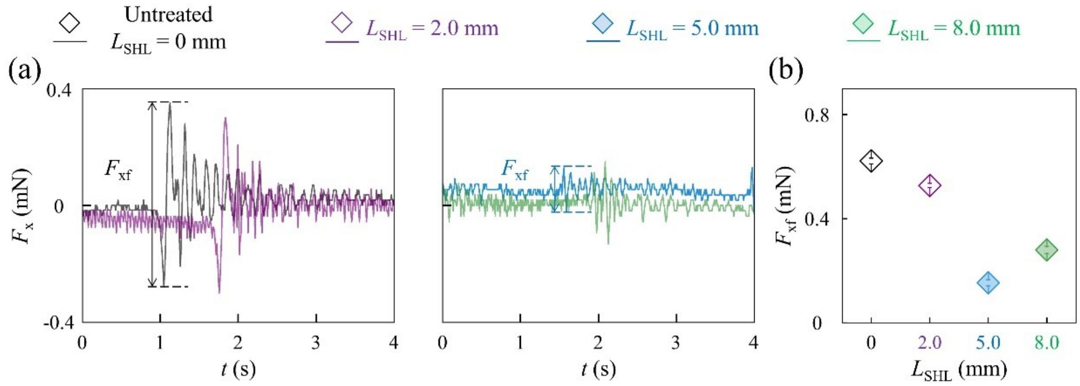

Fig. S12. Horizontal force F_x comparisons of PET sheets. (a) Horizontal force F_x versus time after one dripping for PET sheets with different bottom L_{SHL} treatments at Q = 2.0 mL/min. (b) The maximum force amplitudes F_{xf} versus PET sheets with different bottom L_{SHL} treatments. All error bars are the ± SD (n = 5) and they are smaller than the symbols.

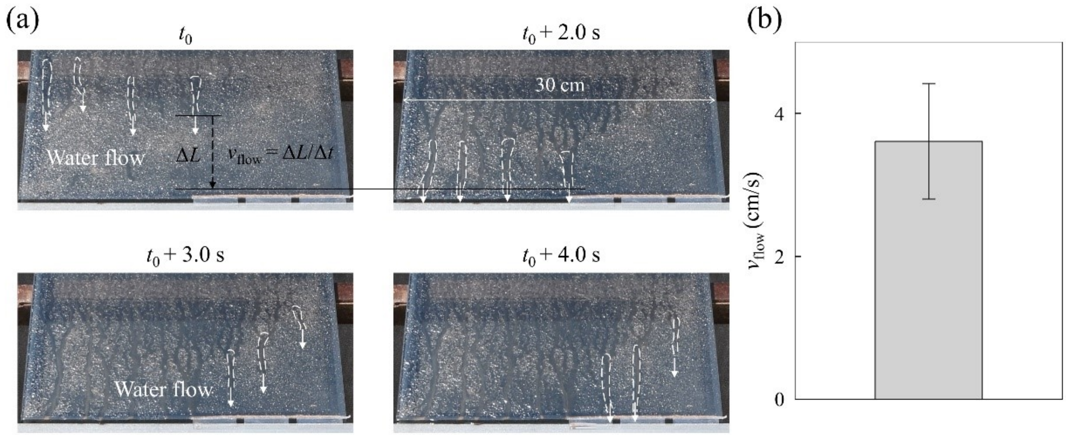

Fig. S13. Water flow speed characterizations. (a) Selected snapshots demonstrates water flows gradually flow downwards. Water flow speed can be express as $v_{flow} = \Delta L/\Delta t$. (b) Calculated results of water flow speed v_{flow}.

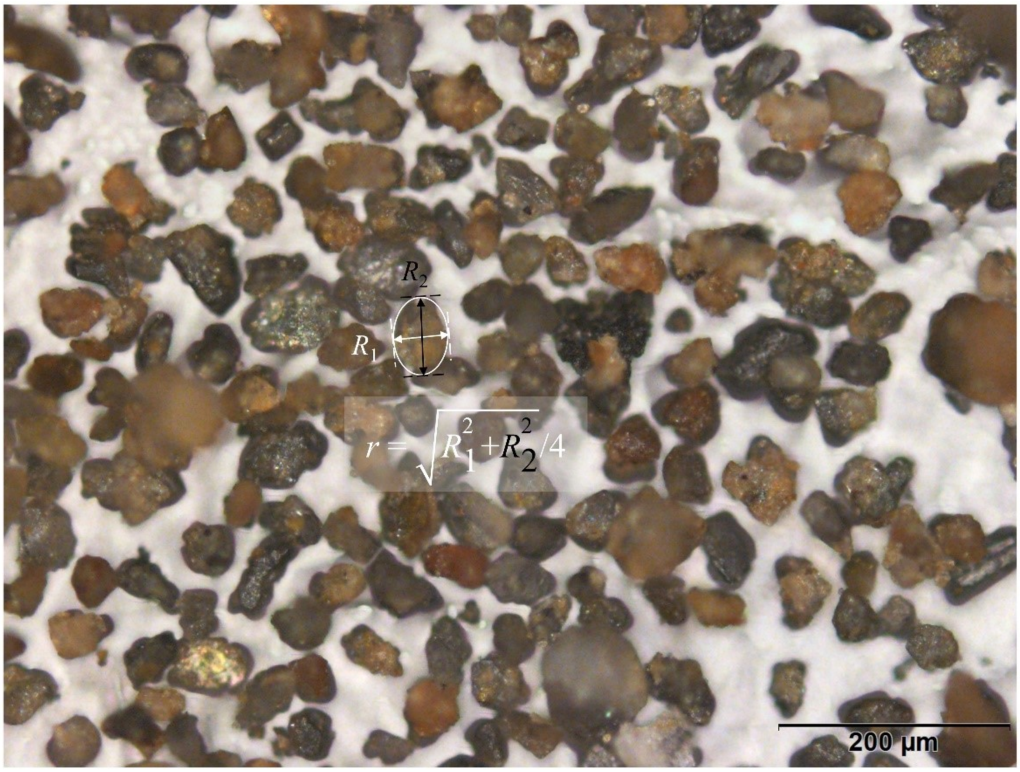

Fig. S14. Microphotograph of dust particles characterizes their sizes.

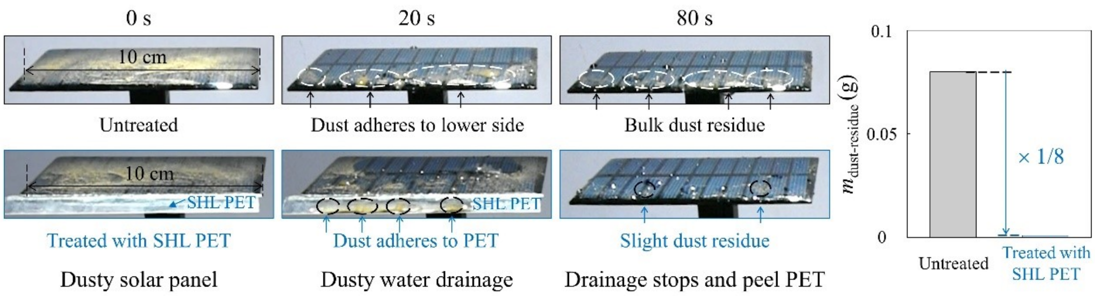

Fig. S15. Dedusting demonstration for solar panels. (a) Selected snapshots of the dedusting process for untreated solar panel and treated solar panel with a superhydrphilic PET sheet of 10 cm x 1 cm, respectively. (b) Dust residue mass characterizations.

Movie S1. Two drainage models for *Pontederia crassipes* leaf.

Movie S2. Comparisons of the two drainage models.

Movie S3. Drainage planes under realistic rainfall environment.

Movie S4. Dusty water drainage on various materials.